Preexisting helminth infection induces inhibition of innate pulmonary anti-tuberculosis defense by engaging the IL-4 receptor pathway

Julius A. Potian,[1,2] Wasiulla Rafi,[1,2] Kamlesh Bhatt,[1,2] Amanda McBride,[1,2] William, C. Gause,[1,3] and Padmini Salgame[1,2]

[1]Department of Medicine, [2]Center for Emerging Pathogens, and [3]Center for Immunity and Inflammation, University of Medicine and Dentistry of New Jersey, Newark, NJ 07101

Tuberculosis and helminthic infections coexist in many parts of the world, yet the impact of helminth-elicited Th2 responses on the ability of the host to control *Mycobacterium tuberculosis* (Mtb) infection has not been fully explored. We show that mice infected with the intestinal helminth *Nippostrongylus brasiliensis* (Nb) exhibit a transitory impairment of resistance to airborne Mtb infection. Furthermore, a second dose of Nb infection substantially increases the bacterial burden in the lungs of co-infected mice. Interestingly, the Th2 response in the co-infected animals did not impair the onset and development of the protective Mtb-specific Th1 cellular immune responses. However, the helminth-induced Th2 environment resulted in the accumulation of alternatively activated macrophages (AAMs) in the lung. Co-infected mice lacking interleukin (IL) 4Rα exhibited improved ability to control Mtb infection, which was accompanied by significantly reduced accumulation of AAMs. Moreover, IL-4Rα$^{-/-}$ mice adoptively transferred with wild-type macrophages had a significantly higher Mtb load in their lungs compared with those that received IL-4Rα$^{-/-}$ macrophages, suggesting a direct contribution for the IL-4R pathway to the heightened susceptibility of co-infected animals. The Th2 response can thus enhance the intracellular persistence of Mtb, in part by mediating the alternative activation of macrophages via the IL-4Rα signaling pathway.

CORRESPONDENCE
Padmini Salgame:
salgampa@umdnj.edu

Abbreviations used: AAM, alternatively activated macrophage; BMDM, BM-derived macrophage; CAM, classically activated macrophage; Mtb, *Mycobacterium tuberculosis*; Nb, *Nippostrongylus brasiliensis*; NOS, nitric oxide synthase; TB, tuberculosis.

It is estimated that tuberculosis (TB) infects one third of the world's population, resulting in two million deaths per year (World Health Organization, 2008). In addition, helminthic infections are estimated to occur in 1.5 billion people worldwide and a great majority of those infections are concentrated in developing nations where TB is endemic (Bethony et al., 2006; Brooker et al., 2006). Given the overlapping geographic distribution of helminths and *Mycobacterium tuberculosis* (Mtb) infections, the importance of investigating whether a lung-dwelling helminth can potentially thwart the ability of the host to handle pulmonary Mtb infection cannot be undermined.

A hallmark of helminthic infections, both in experimental models and human infection is the generation of profound T helper (Th) 2 and T regulatory cell responses (Sher et al., 1991; McKee and Pearce, 2004; Anthony et al., 2007) that have the potential to impede Th1 cell development. Indeed, several studies have reported that helminth infections can alter the immune response elicited by the host to other invading pathogens (Actor et al., 1993; Pearlman et al., 1993; Helmby et al., 1998; Rodríguez et al., 1999). Chronic worm infection of mice reduces immunogenicity (Elias et al., 2008) and protective efficacy of Bacillus Calmette Guérin (BCG) vaccination against Mtb (Elias et al., 2005). Children with onchocerciasis exhibit lowered cellular responses to purified protein derivative antigens (Stewart et al., 1999) and infants respond poorly to BCG vaccination if the mothers had filarial and schistosomal infections during pregnancy (Malhotra et al., 1999). Coincident helminth infection is also associated with reduced Th1 responses in active (Resende Co et al., 2007) and latent (Babu et al., 2009)

The Rockefeller University Press $30.00
J. Exp. Med.
www.jem.org/cgi/doi/10.1084/jem.20091473

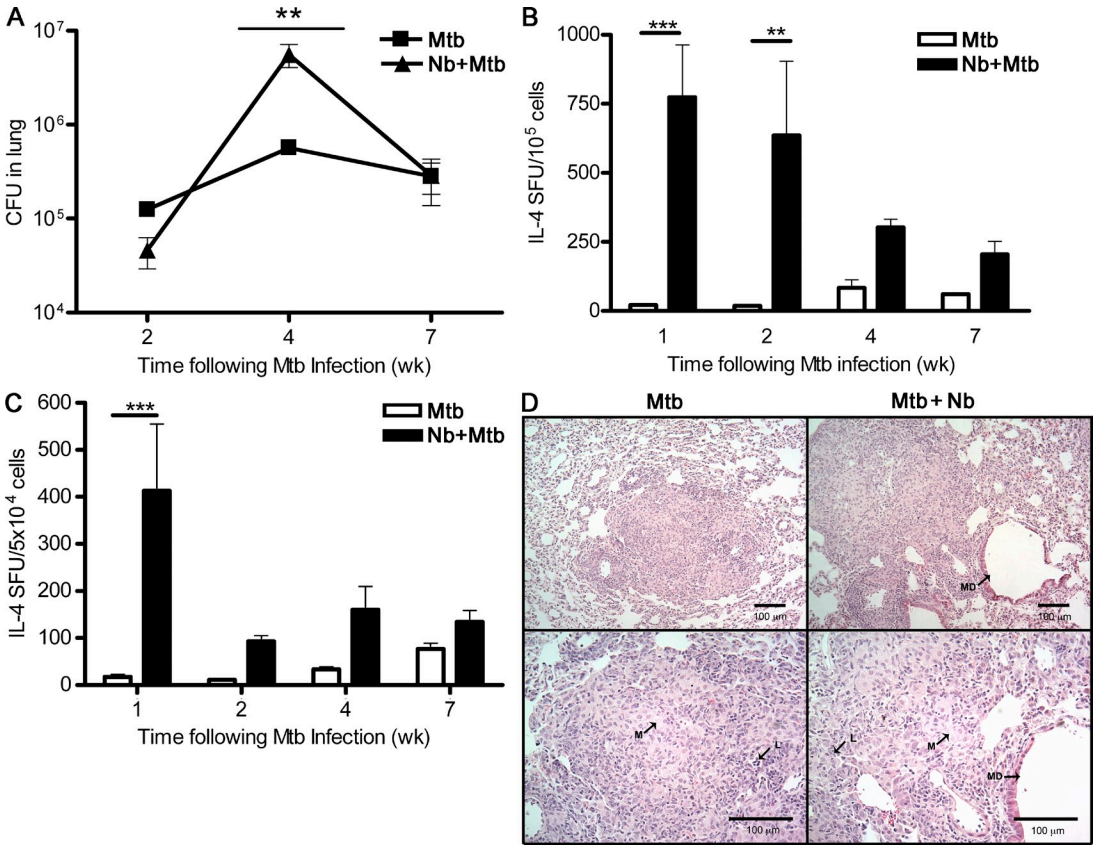

Figure 1. Co-infection alters resistance of host to Mtb infection. BALB/c mice were either injected s.c. with 500 Nb L3 larvae 5 d before infection with ∼100 viable CFU of the virulent Erdman strain of Mtb via aerosolization or were infected with Mtb alone. At the indicated time intervals after Mtb infection, mice were sacrificed and lungs and draining mediastinal LNs were harvested. (A) Viable organisms in the lungs were determined by plating serial dilutions of lung homogenates for CFU. Data are presented as mean CFU counts ± SD. Data are representative of one of three independent experiments (n = 5 mice/group/time point). (B and C) Single cell suspensions of LNs (B) and lungs (C) were stimulated in duplicate with anti-CD3 and anti-CD28 antibodies and IL-4–secreting cells were quantified by ELISPOT. Spot forming units (SFU) were counted using an ImmunoSpot reader. Data are presented as mean SFU ± SD. Data are representative of two independent experiments. **, $P < 0.01$; ***, $P < 0.001$. (D) Histopathological evaluation of H&E-stained sections was performed on formalin-fixed paraffin-embedded tissues from the lungs of mice obtained at 4 wk after aerosol infection with ∼100 CFU of Mtb. Representative photomicrographs are shown. Tissue from four individual mice from each group was compared for the presence of granuloma formation and cellular infiltration. Arrows denote the following: MD, Nb-induced mechanical damage; L, lymphocyte; M, foamy macrophage.

TB. Clearly, there is accumulating literature on the interaction of helminths with mycobacteria, but none of these studies fully explored the mechanistic basis for how helminth-modulated immune response has an impact on host control of Mtb infection.

Nippostrongylus brasiliensis (Nb) is a mouse prototype of human intestinal nematodes such as *Ascaris lumbricoides* and *Strongyloides stercoralis*, which reside briefly in the lungs as a part of their life cycle. Upon subcutaneous injection, the infective third stage (L3) larvae of Nb migrate to the lungs as early as 11 h via the subcutaneous tissue vasculature. A subsequent molt occurs in the lung between 19 and 32 h with the L4 larvae remaining in the lungs up to 50 h after infection before being regurgitated via the trachea to the intestinal tract, where they mature into adult worms. During the transient migration through the lung, the parasite induces a strong localized Th2 response in the lung and associated draining LNs. The lungs also show an elevated expression of AMCase (acidic mammalian chitinase), Fizz-1 (found in inflammatory zone; also known as resistin-like molecule α or RELM-α), and Ym1, hallmarks of an alternative phenotypic activation of macrophages which are also referred to as M2 macrophages (Mosser and Edwards, 2008). The L3 larvae also migrate from the skin to the lungs during reinfection but undergo severe attrition in the lung as a result of the induction of a rapid and strong CD4 Th2 response. This is also associated with significantly reduced worm fecundity in the lungs and gut of reinfected mice. (Harvie et al., 2010).

In the current study, we co-infected mice with Nb and Mtb to explore whether the immunological environment created by a preexisting helminth infection would have a negative impact on the host protective responses against an aerosol infection with Mtb. We present evidence that pulmonary immune changes caused by helminth result in enhanced susceptibility to TB. Data presented also point out that alternatively

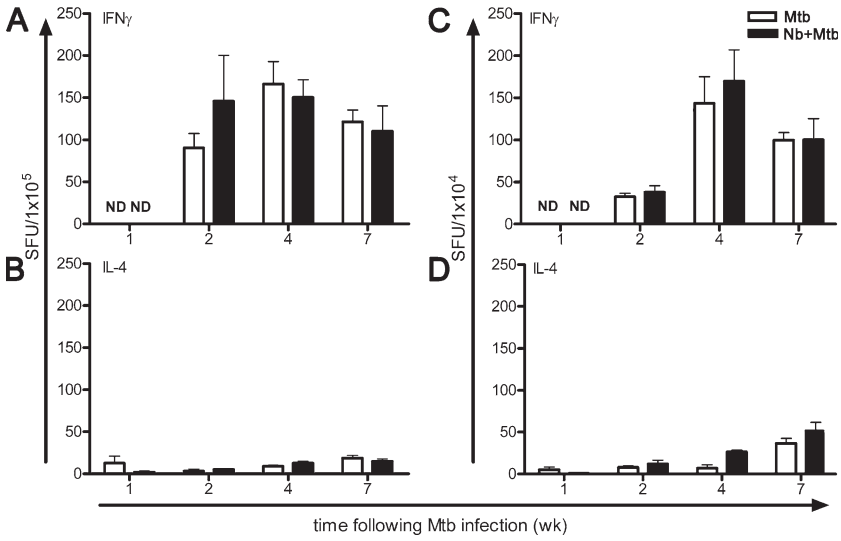

Figure 2. Equivalent frequency of Mtb-specific IFN-γ–secreting cells in co-infected and Mtb-alone–infected mice. Mtb-specific secretion of IFN-γ (top) and IL-4 (bottom) by total LN (A and B) and lung (C and D) cells isolated at indicated time points after infection was determined by ELISPOT using Mtb-pulsed dendritic cells as antigen-presenting cells. Data are presented as mean SFU ± SD. Data are representative of two independent experiments (n = 5 mice/group). ND, not detected.

activated macrophages (AAMs) constitute a major cellular pathway that compromises the helminth-infected host's ability to restrict Mtb growth.

RESULTS

Nb infection induces a strong Th2 response in the lung and transitory impairment of resistance to airborne Mtb infection

Previous studies have shown that between 5 and 7 d after Nb infection, there is a transient but potent Th2 response in the lung and mediastinal LNs of infected mice (Liu et al., 2002). Therefore, groups of BALB/c mice were either left uninfected or were infected subcutaneously with 500 L3 stage Nb larvae and, 5 d later, both groups were challenged by the aerogenic route with 100 CFU of the virulent Erdman strain of Mtb. Bacterial burden, T cell, and granulomatous response in the lung was compared at different time intervals between co-infected mice receiving both Nb and Mtb infections (Nb+Mtb) and mice receiving Mtb infection alone (Mtb).

At 2 wk after Mtb infection, the Mtb load in the lungs of the two groups of mice was similar. However, at week 4, the Mtb burden in co-infected mice was significantly higher in comparison with the group infected with Mtb alone. Interestingly, this increase in Mtb burden in the lungs of co-infected animals was transient, and by week 7 the bacterial burden in the co-infected mice decreased and was comparable to Mtb-alone mice (Fig. 1 A). Furthermore, the increased bacterial burden correlated with a robust Th2 response in the co-infected animals. Compared with mice receiving Mtb infection alone, co-infected mice had a significantly higher number of total IL-4–secreting cells in the LN at weeks 1 and 2 in the infection, which declined as infection progressed (Fig. 1 B). Similarly, the lungs of co-infected animals had significantly higher IL-4–producing T cells compared with mice infected with Mtb alone (Fig. 1 C). The peak response was seen at week 1, after which IL-4–secreting T cell numbers declined and stayed at the same level through week 7. Although relatively few lL-4–secreting cells were found in the lungs of Mtb-alone mice at weeks 2 and 4 of infection, it is worth noting that there was a modest, albeit significant, increase at week 7 of infection.

Formation of a tubercle granuloma is integral to protective immunity and containment of infection (Co et al., 2004). We next assessed whether co-infection led to changes in lung histopathology and granulomatous response. Despite the increase in bacterial burden and mechanical damage induced by the Nb larvae, histologically the granulomas of 4-wk–co-infected mice were not noticeably different than those of Mtb-alone–infected mice. Both groups displayed characteristic granuloma architecture with a lymphocytic core and presence of numerous activated macrophages (Fig. 1 D)

Development of Mtb-specific Th1 response is not impaired in co-infected animals despite a strong Th2 environment

Th2 cytokines have been shown to inhibit Th1 polarization and function (Le Gros et al., 1990; Hsieh et al., 1993; Seder et al., 1993). We therefore argued that in co-infected animals, the Nb-specific Th2 response may interfere with the development of Mtb-specific Th1 response and thereby diminish Th1-mediated anti-mycobacterial activity in the lungs. To determine if this was the case, we measured by ELISPOT the frequency of Mtb-specific IL-4– and IFN-γ–secreting T cells. Analysis of mediastinal LN cells from the two groups of mice showed that the frequency of Mtb-specific IFN-γ–secreting cells was comparable in both the groups (Fig. 2 A). Additionally, no Mtb-specific IL-4–secreting cells were observed in the co-infected animals (Fig. 2 B), indicating that the Nb-induced IL-4 response was not pushing Mtb-specific T cell differentiation toward the Th2 pathway. Analysis of infected lungs paralleled the findings observed in the LN, with no difference seen in the frequency of Mtb-specific IFN-γ–secreting (Fig. 2 C) and IL-4–secreting (Fig. 2 D) cells between the two infection groups. Interestingly, there was a small but significant increase in IL-4–secreting T cells in both groups of animals at 7 wk after infection. Collectively, these results indicate that in co-infected animals, despite a strong Nb-induced Th2 response in the LN, Mtb-specific Th1 polarization occurs unabated in the LN with associated recruitment of the polarized Th1 cells to the lung.

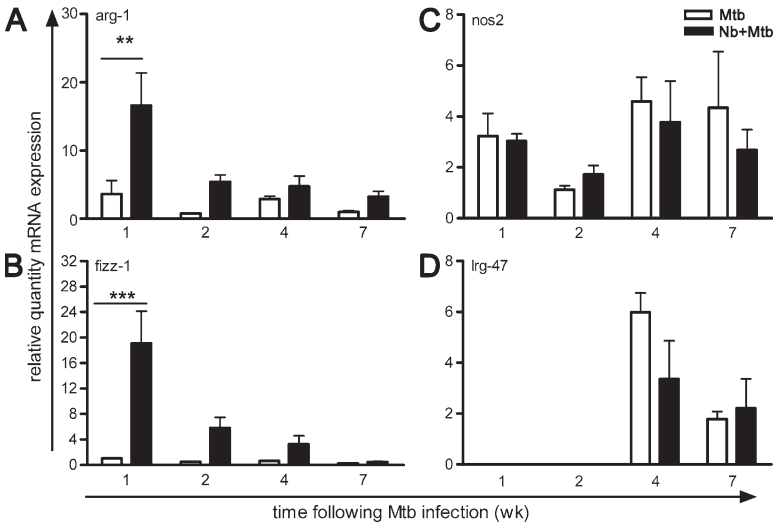

Figure 3. Gene expression of AAM markers is elevated in lungs of co-infected mice. Total RNA was isolated from infected lungs of mice co-infected with Nb and Mtb or infected with Mtb alone at the indicated time points after Mtb infection. Gene expression of *arg-1* (A), *fizz-1* (B), *nos2* (C), and *lrg-47* (D) was assessed by RT PCR. The relative expression of the gene of interest was determined as the ΔCt, relative to the message of the housekeeping gene β-actin. The change in relative message levels (relative quantity) to that expressed in uninfected lungs was calculated as the ΔΔCt. Data are presented as mean ± SD. Data are representative of two independent experiments (n = 5 mice/group). **, P < 0.01; ***, P < 0.001.

Impaired resistance of Nb-infected mice to Mtb is mediated by AAMs

Macrophage activation can be divided into Th1-mediated classical and Th2-mediated alternative pathways (Martinez et al., 2009). Classically activated macrophages (CAMs) up-regulate nitric oxide synthase (NOS) 2, which oxidizes L-arginine to NO and citrulline. NO promotes killing of intracellular Mtb (Chan et al., 1992; MacMicking et al., 1997). In contrast, arginase-1 (ARG-1) expression is induced in AAMs, and the enzyme hydrolyzes the same substrate L-arginine to urea and L-ornithine. Germane to this study, AAMs are compromised in their ability to kill Mtb (Harris et al., 2007). Indeed, mice lacking *arg-1* exhibit a reduction in lung bacterial burden in comparison with WT mice (El Kasmi et al., 2008). Given that NOS2 and ARG-1 compete for the same substrate, inhibit each other's expression, and are functionally divergent in their ability to control Mtb replication, it is reasonable to speculate that the increased Mtb burden in the lungs of co-infected mice could result from either ARG-1–induced down-modulation of NOS2 or abrogation of antimicrobial function of CAMs. We next sought to determine how the mixed Th1 and Th2 microenvironment of co-infected lungs affected macrophage activation. As shown in Fig. 3, transcripts for *arg-1* (Fig. 3 A) and *fizz-1* (Fig. 3 B), markers of AAMs, were significantly elevated only in the lungs of co-infected mice. Paralleling IL-4 expression, the highest expression for *arg-1* and *fizz-1 was* observed at week 1, after which gene expression diminished. Surprisingly, equivalent expression of *nos2* (Fig. 3 C) and *lrg-47* (Fig. 3 D), genes corresponding to CAMs, was observed in the lungs of both groups of mice at all time points tested. Matching the IFN-γ expression pattern, *nos2* and *lrg*-47 expression was highest at 4 wk and remained elevated at 7 wk after infection.

The data so far indicate that the initial bacterial growth in co-infected mice is akin to mice infected with Mtb alone, despite their lung milieu being AAM dominated at early time points after infection. In the co-infected mice, an increase in bacterial burden becomes apparent only at 4 wk of infection. Although, as expected, at ∼4 wk of infection when Th1 responses peak, Mtb-alone–infected mice are able to contain their infection and maintain a steady bacterial load. We reasoned that in co-infected animals, Mtb continues to grow unrestricted for a longer time because more Mtb is residing in AAMs that are not efficient at killing Mtb. It is further likely that as IL-4 responses taper and reciprocal elevation of IFN-γ expression gradually occurs in the lungs of co-infected animals, the AAMs in the lungs—harboring Mtb as a result of decreasing pressure from Th2 cytokines—lose their AAM phenotype and are now able to respond to IFN-γ. As such, the AAM-dominated lung milieu in co-infected animals delays the ability of the host to induce a Th1-mediated restriction of Mtb growth. This line of argument is consistent with equivalent ability to control infection at 7 wk in both groups of infected mice.

To ascertain whether AAMs, upon removal of IL-4/IL-13, can respond to IFN-γ and that alternative activation is not a terminally differentiated state, we performed an in vitro survival assay. BM-derived macrophages (BMDMs) were either left unstimulated, stimulated with IFN-γ to induce CAMs,

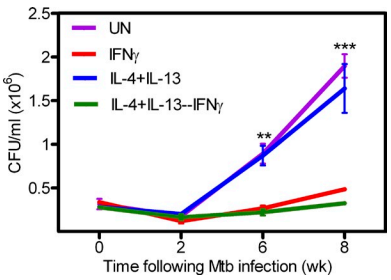

Figure 4. AAM can respond to IFN-γ in vitro. BMDMs were left untreated (UN) or were activated with 20 ng/ml IL-4 + 10 ng/ml IL-13 or 100 U/ml IFN-γ for 18 h. Macrophages were infected with Erdman Mtb at an MOI of 1 for 5 h, treated with 200 µg/ml amikacin for 1 h, and washed. 100 U/ml IFN-γ was added to one half of the IL-4 + IL-13–treated macrophages (IL-4+IL-13–IFNγ). At the indicated time points, macrophages were lysed and serial dilutions plated for CFU. Data are presented as mean CFU counts ± SD. Data are representative of two independent experiments. **, P < 0.01; ***, P < 0.001.

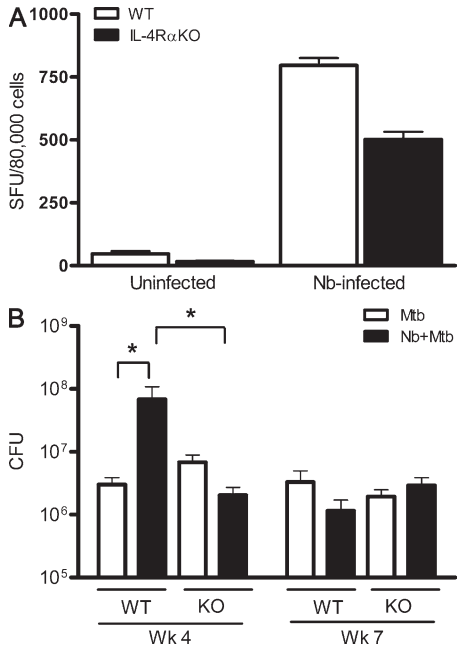

Figure 5. Co-infected mice do not exhibit increased Mtb burden in the absence of IL-4Rα signaling. (A) Lungs from uninfected and Nb-infected WT or IL-4Rα$^{-/-}$ (KO) mice were harvested 5 d after Nb infection, single cell suspensions of lungs were stimulated in triplicate with anti-CD3 and CD28 antibodies, and IL-4–secreting cells were quantified by ELISPOT. Data are presented as Spot forming units (SFU) ± SD (n = 4 mice/group). (B) Viable organisms in the lungs were determined at the indicated times by plating serial dilutions of lung homogenates for CFU. Data for weeks 4 and 7 are pooled from two independent experiments (n = 7–8 mice /group) and presented as mean CFU counts ± SD. *, $P < 0.05$.

or stimulated with IL-4 and IL-13 to induce AAMs. The cultures were then infected with Mtb and, 5 h later, washed to remove extracellular Mtb. To mimic the in vivo decrease in Th2 cytokines and increase in IFN-γ, some wells of the Mtb-infected IL-4 and IL-13 cultures were exposed to IFN-γ. At subsequent time intervals, macrophages were lysed and plated for CFU. Analysis of Mtb survival showed no difference in CFU at day 0, indicating that Mtb uptake was similar in all the infected groups. No difference in CFU was seen even at 2 d after Mtb infection, but by days 6 and 8, a significant increase in bacterial count was seen in untreated and AAMs in comparison to CAMs (Fig. 4). Importantly, addition of IFN-γ to AAMs after Mtb infection led to reduction in CFU counts at days 6 and 8 (Fig. 4), indicating that after removal of Th2 cytokines, AAMs are able to respond to a Th1 milieu. This supports our argument that in co-infected animals, the presence of AAMs provides a niche for Mtb when the lung milieu is Th2 dominant, but as the Th2 response wanes the AAMs slowly begin to respond to the anti-mycobacterial effects of IFN-γ.

We next determined whether inhibiting AAM development would lead to better control of Mtb growth in co-infected mice. Analogous to the findings of previous studies (Jankovic et al., 2000; van Panhuys et al., 2008), we also found that the helminth-induced Th2 response is independent of IL-4Rα signaling. As shown in Fig. 5 A, a significant increase in the number of IL-4–secreting T cells was observed in the lungs of both Nb-infected WT and IL-4Rα$^{-/-}$ mice in comparison with their uninfected counterparts. The fact that Nb-infected IL-4Rα$^{-/-}$ mice have an intact Th2 response but lack the ability to respond to the Th2 cytokines IL-4 and IL-13 provides a model system to test whether there is a causal link between the induction of AAMs and enhanced susceptibility to Mtb in co-infected animals. Ergo, IL-4Rα$^{-/-}$ mice were infected with Nb and Mtb or with Mtb alone. As observed previously at week 4, WT co-infected mice displayed a significant increase in lung bacterial burden. In contrast, a similar increase was not seen in co-infected IL-4Rα$^{-/-}$ mice (Fig. 5 B). By week 7, bacterial burdens in both WT and IL-4Rα$^{-/-}$ mice declined and became comparable with mice infected with Mtb alone (Fig. 5 B). Although not statistically significant, the slightly higher level of bacterial burden seen at week 4 in Mtb-alone–infected IL-4Rα$^{-/-}$ mice is consistent with what has been observed by other groups (Jung et al., 2002).

More significantly, we observed that Nb infection of IL-4Rα$^{-/-}$ mice did not induce the development and accumulation of AAMs in the lungs of co-infected mice. Flow cytometric analysis of lung cells was performed to quantitate the numbers of CAMs and AAMs present in the lungs of infected animals. We used NOS2 expression as a marker of CAM and Fizz-1 expression as a marker of AAMs because ARG-1 staining by flow cytometry proved to be problematic. Lungs were harvested from week 3–infected mice and single cell suspensions were prepared and reacted with antibodies against CD11b, CD11c, NOS2, and Fizz-1 for analysis by multicolor flow cytometry. Cell populations were first gated based on their CD11b and CD11c expression into three subsets: (1) CD11b^{+}c^{-}, (2) CD11b^{-}c^{+}, and (3) CD11b^{+}c^{+} cells which broadly represent interstitial and recruited macrophages, lung alveolar macrophages, and dendritic cells, respectively. NOS2- and Fizz-1–expressing cells were next quantified in each of the gated population. Fig. S1 presents the gating strategy for the three subsets. The dot plots for NOS2 and Fizz-1 expression in each of the subsets is presented in Figs. S2 and S3, respectively. The majority of NOS2-expressing cells were found in the CD11b^{+}c^{-} subset in both co-infected and Mtb-alone–infected mice (Fig. 6 A). Interestingly, equivalent numbers of NOS2-expressing cells were present in both groups of WT mice, whereas in the co-infected IL-4Rα$^{-/-}$ mice, there was a significant increase in NOS2-expressing cells compared with Mtb-alone mice (Fig. 6 A). It is possible that a subset of the NOS2-expressing cells within the CD11b^{+} compartment contains neutrophils. Analysis of Fizz-1 staining showed that, unlike NOS2, the percentage of Fizz-1–expressing cells in each subset was higher in the co-infected group compared with Mtb alone (Fig. 6 B), whereas such an increase was not seen in co-infected IL-4Rα$^{-/-}$ mice (Fig. 6 B). However, it must be noted that the CD11b^{+}c^{-} subset contained the highest percentage of Fizz-1–expressing cells (Fig. S3).

Further supporting the lack of AAM development in the absence of IL-4Rα, analysis of ARG-1 activity in lung lysates showed significantly increased ARG-1 activity in WT co-infected mice at 3 wk compared with Mtb alone, whereas the activity was significantly less in co-infected IL-4Rα$^{-/-}$ mice (Fig. 6 C).

The results of immunohistochemical staining of lung tissue sections for NOS2 and ARG-1 protein presented in Fig. 6 D show that NOS2-positive cells are present in WT and IL-4Rα$^{-/-}$ lung granulomas of both co-infected and Mtb-infected mice. In contrast, and consistent with ARG-1 activity, accumulation of ARG-1–positive cells was restricted to lung granulomas of co-infected WT mice only. No ARG-1–positive staining was discernible in lung sections from WT and IL-4Rα$^{-/-}$ mice infected with Mtb alone and also from co-infected IL-4Rα$^{-/-}$ mice. In agreement with mRNA levels, cells expressing ARG-1 protein went down at 7 wk in WT co-infected mice (unpublished data).

Next, WT or IL-4Rα$^{-/-}$ macrophages were adoptively transferred into IL-4Rα$^{-/-}$ mice to create two groups of chimeric mice that differed only at the level of having a subset of macrophages either capable of differentiating into AAMs, or not, during Nb infection. Our strategy of adoptively transferring macrophages into the IL-4Rα$^{-/-}$ background, where host susceptibility to Mtb is not modulated by Nb co-infection, provided us with an ideal system to demonstrate that AAMs activated via the IL-4R pathway are likely to be responsible for the enhanced Mtb burden observed in the co-infected animals. Thioglycollate-elicited CFSE-labeled WT or IL-4Rα$^{-/-}$ peritoneal macrophages were intratracheally instilled into IL-4Rα$^{-/-}$ mice (10×10^6 cells instilled per mouse) and lungs were harvested right before Nb infection or 5 d after Nb infection. CFSE-positive cells were present in equivalent numbers at both time points in the lungs of the two groups of chimeric mice, demonstrating that the instilled macrophages home to the lungs and persist in the tissue

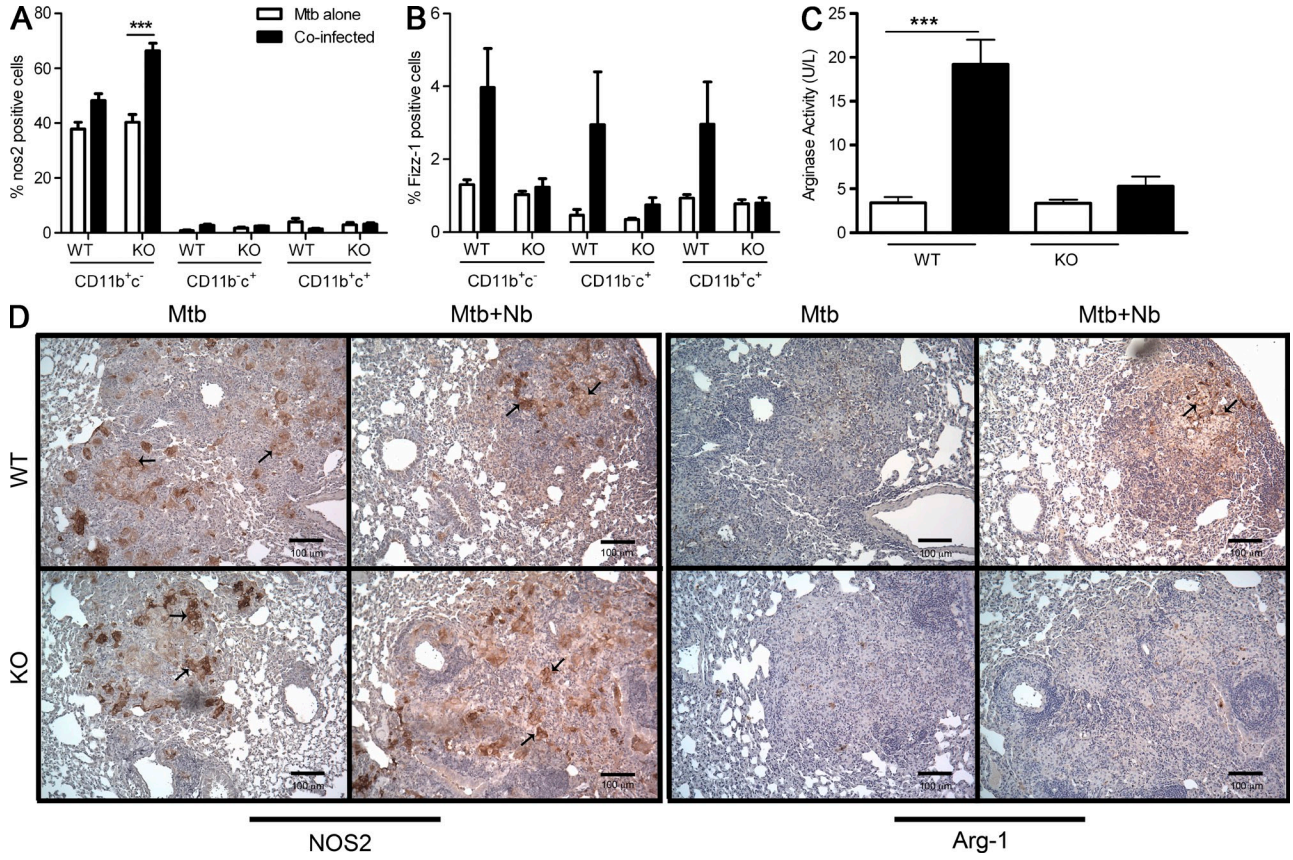

Figure 6. Loss of AAMs in lungs of co-infected mice in the absence of IL-4Rα. (A and B) WT and IL-4Rα$^{-/-}$ (KO) mice infected or not with Nb were aerosol infected with ∼100 CFU of Mtb. Cells were isolated from infected lungs at 3 wk after Mtb infection and stained with fluorescently conjugated antibodies for intracytoplasmic expression of nos2 (A) and Fizz-1 (B) and cell surface expression of CD11b and CD11c. The cells were acquired by flow cytometry. The data are expressed as percentages of nos2 (A) and Fizz-1 (B) cells present in the CD11b$^+$, CD11c$^+$, and CD11b$^+$c$^+$ gated population. (C) Lungs lysates from WT or IL-4Rα$^{-/-}$ Mtb-alone or co-infected lungs 3 wk after Mtb infection were collected and analyzed for arginase activity as described in Materials and methods. Data in A–C are representative of two independent experiments (n = 5 mice/group) and are presented as mean ± SD. ***, P < 0.001. (D) IHC staining for nos2 and Arg-1 protein was performed on formalin-fixed paraffin-embedded tissues from the lungs of mice obtained 4 wk after aerosol infection with ∼100 CFU of Mtb. Tissue from four individual mice from each group was compared. The figure presents representative photomicrographs. Arrows indicate areas of positive staining.

(Fig. S4). On day 5 after Nb infection, there was a robust yet equivalent *IL-4* gene expression in the lungs from both groups of chimeric mice (Fig. 7 A). However, there was a modest but significant difference in *arginase1* mRNA expression between mice receiving WT macrophages compared with those receiving IL-4Rα$^{-/-}$ macrophages (Fig. 7 B). Together, these findings indicate that the adoptively transferred WT macrophages differentiate to AAM in response to the Th2 environment in the Nb-infected IL-4Rα$^{-/-}$ host. Consistent with the differential arginase expression, comparison of Mtb growth in the two groups of Nb-infected chimeric mice showed that mice receiving WT macrophages had a significantly higher Mtb load in the lungs compared with their counterparts receiving IL-4Rα$^{-/-}$ macrophages (Fig. 7 C). The ∼1 log difference in bacterial burden between the two groups of mice is similar to what was observed between WT mice receiving Mtb alone and co-infected animals, indicating that susceptibility was restored to WT levels in the transfer experiments. These data directly establish that IL-4Rα–mediated alternative activation of macrophages markedly contributes to the increased bacterial burden in the lungs of co-infected animals.

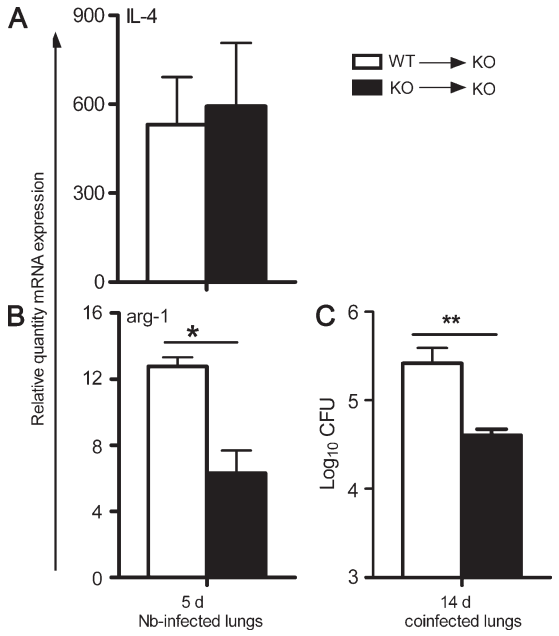

Figure 7. Adoptive transfer of WT macrophages to Nb-infected IL-4RαKO mice enhances Mtb growth in lungs. 10 × 10^6 thioglycollate-elicited peritoneal macrophages from WT or IL-4Rα$^{-/-}$ (KO) mice were adoptively transferred via the intratracheal route into IL-4Rα$^{-/-}$ hosts and infected with Nb the next day. 5 d later, both groups of mice were infected with Mtb. Five mice from each group were sacrificed before Mtb infection to determine the gene expression of *IL-4* (A) and *arg-1* (B) by RT PCR in the lungs. The relative expression of the gene of interest was determined as the ΔCt relative to the message of the housekeeping gene β-actin. The change in relative message levels (relative quantity) compared with that expressed in uninfected lungs was calculated as the ΔΔCt. Evaluation of Mtb burden in lungs of co-infected animals (five mice in each group) was determined at 2 wk after Mtb infection (C). Data are presented as mean ± SD. Data are representative of two independent experiments. *, P < 0.05; **, P < 0.01.

Sustained Th2 response leads to exacerbation of TB disease in co-infected animals

In endemic areas, the likelihood of parasitic reinfections is high. We therefore argued that two Nb infections may enhance the Th2 response and AAM development leading to a more sustained increase in Mtb burden in the lung. As before, we injected BALB/c mice subcutaneously with 500 L3 stage Nb larvae, and 5 d later the mice were infected aerogenically with Mtb. 5 d after Mtb infection, mice were injected with a second round of Nb larvae. Comparative evaluation of lung lysates at 3 wk after Mtb infection showed higher arginase activity in co-infected mice that had received 2 Nb infections (200 ± 3 U/liter) versus those that had received single Nb infection (75 ± 6 U/liter). Consistent with higher arginase activity, double infection with Nb led to approximately a 2-log

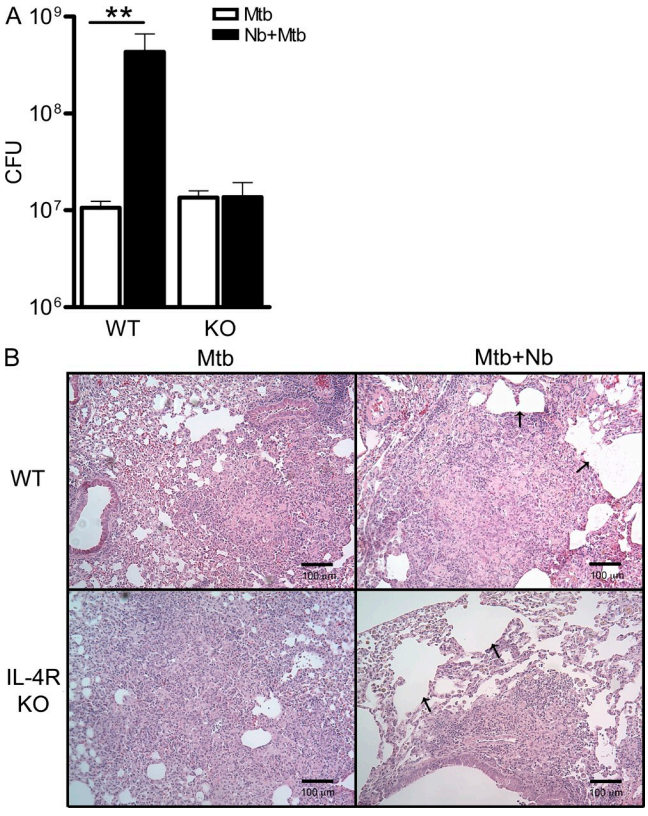

Figure 8. Two Nb infections lead to enhanced susceptibility to Mtb infection. (A) WT and IL-4Rα$^{-/-}$ mice were either infected with 500 CFU Mtb alone or infected with ∼500 Nb L3 larvae s.c 5 d before and again 5 d after Mtb infection (n = 4 mice/group). At day 21 after infection, viable organisms in the lungs were determined by plating serial dilutions of lung homogenates for CFU. Data are presented as mean CFU counts ± SD. **, P < 0.01. (B) Lung sections were formalin-fixed and paraffin-embedded at day 21 after Mtb infection. The figure presents representative photomicrographs (n = 4 mice/group). Arrows denote Nb-induced mechanical damage. Data are representative of two independent experiments.

higher level of bacterial burden in co-infected mice (Fig. 8 A). Of note was the observation that double Nb-infected mice died by 5 wk after Mtb infection, suggesting an inability of these mice to control Mtb infection (unpublished data). Histological analysis of granuloma architecture at 3 wk after Mtb infection revealed that the size of the granuloma of double Nb-infected mice was noticeably larger than Mtb-alone mice, possibly as a result of the greatly increased bacterial burden (Fig. 8 B). Extensive mechanical damage was also evident in the lungs of double Nb-infected mice (Fig. 8 B). To confirm that mechanical damage was not the main cause of increased severity of disease in the double Nb-infected mice, we examined in parallel the consequence of Nb double infection in IL-4Rα$^{-/-}$ mice. IL-4Rα$^{-/-}$ mice injected twice with Nb had lung bacterial burdens that were comparable with WT Mtb-alone levels (Fig. 8 A), despite extensive damage to lung (Fig. 8 B). Overall, these results indicate that IL-4R–mediated development of AAMs enhanced morbidity and mortality in co-infected animals.

DISCUSSION

Helminth infections are highly prevalent in populations where Mtb infection is endemic, and it has been widely conjectured that the strong mucosal Th2 and T regulatory cell responses elicited by these parasites can down-modulate protective immune reactions against Mtb. However, no study so far has addressed causality versus coincidence and determined whether helminth infections in fact affect the pathogenesis of TB and the ability of the host to restrict Mtb growth. The findings from the present study strongly indicate that helminthic infections compromise the host's ability to control Mtb infection via a mechanism involving alternative activation of lung macrophages.

It was rather surprising to observe that despite a strong Th2 response in the LN, Mtb-specific Th1 cell development and recruitment to the lungs remained unhampered in co-infected animals. Consistent with contemporaneous induction of both Th1 and Th2 cells in the lungs of co-infected animals, analysis of downstream macrophage activation showed the presence of both CAMs and AAMs. However, enhanced Mtb growth occurred in co-infected animals only when there was an ongoing Th2 response driving the accumulation of AAMs in the lungs. As the Nb larvae migrate out of the lungs and expression of IL-4, ARG-1, and Fizz-1 subsided, the animals gained the ability to control Mtb infection, akin to animals infected with Mtb alone. It should be noted that unlike the long-term changes observed in the lungs of mice infected with Nb alone (Reece et al., 2008), co-infected mice rapidly down-regulate expression of IL-4 and markers characterizing AAMs.

Nb infection induces physical damage to the lung caused by larval migration (Marsland et al., 2008; Reece et al., 2008), and so one could attribute the enhanced Mtb growth observed in co-infected animals to the overall deterioration of lung function and not specifically to AAMs. However, the fact that co-infected IL-4Rα$^{-/-}$ mice were able to restrict Mtb growth akin to mice infected with Mtb alone, despite the physical trauma, suggests evidence to the contrary. Furthermore, co-infected IL-4Rα$^{-/-}$ mice also generated a strong Th2 response, but in contrast to WT co-infected animals failed to express markers associated with AAMs. Results from the adoptive transfer experiment strengthen the paradigm that IL-4R signaling on macrophages and AAM differentiation contributes significantly to the increased Mtb load in the lungs of co-infected animals. Nevertheless, the findings do not rule out the possibility that larvae-induced mechanical damage may be important in initiating an innate IL-4 response and activation of AAMs. In this regard, Loke et al. (2007) have shown in a surgical implant model with *Brugia malayi* that tissue injury by itself is sufficient to transiently induce AAMs in a IL-4Rα signaling-dependent but adaptive Th2 response-independent manner. *B. malayi* infection was, however, necessary to sustain the alternative activation of macrophages. Although the study (Loke et al., 2007) did not identify the source of the innate IL-4 triggering the response, it suggested that it could be from either eosinophils or mast cells. Similarly, in the co-infection model used in this study the tissue damage induced by Nb larvae migrating through the lung parenchyma could be a contributing factor, along with IL-4R signaling, to the activation of AAMs. Future studies are needed to determine if other pathways such as chitin (Satoh et al., 2010) and MyD-88 (Qualls et al., 2010) also contribute to AAM development during co-infection.

AAMs have been shown to abrogate host protection against other intracellular infections. Indeed, conditions that activate AAMs in the lungs of *Cryptococcus neoformans*–infected mice result in the loss of ability of mice to control infection (Arora et al., 2005; Müller et al., 2007). Similarly, in the mouse model of leishmaniasis, disease progression in the highly susceptible BALB/c mice could be significantly delayed by removal of IL-4/IL-13Rα signaling on macrophages and consequent activation of the cells to the alternative phenotype (Hölscher et al., 2006). AAMs also support the growth of *Francisella tularensis* (Ft), and the live vaccine strain of Ft switches macrophage activation from a classical to AAM state (Shirey et al., 2008). In response to *Yersinia enterocolitica* infection, resistant mice activated CAMs, whereas susceptible mice induced AAMs (Tumitan et al., 2007). Co-infection involving the mouse helminth *Heligmosomoides polygyrus* and the Th1-eliciting bacteria *Citrobacter rodentium* demonstrated accumulation of AAMs in co-infected animals and impaired killing of internalized bacteria by these macrophages (Weng et al., 2007). In contrast, LysM^{cre}IL-4Rα$^{flox/-}$ mice that lack IL-4R on macrophages are highly susceptible to acute schistosomiasis as they are unable to activate AAMs. The study showed that these mice do not develop AAMs and consequently develop an enhanced Th1 response, elevated NOS2 expression, and inability to prevent *Schistosoma mansoni* egg–induced inflammation (Herbert et al., 2004). Similarly, Mtb infection also induces a proinflammatory response in the lung, and it has been argued that as infection progresses, immunoregulatory responses are generated to prevent collateral damage to lung

tissue. In contrast to the schistosome study, Mtb-infected mice did not exhibit enhanced immunopathology in the IL-4Rα$^{-/-}$ mice despite lack of AAM development. Perhaps other immunoregulatory circuits control immune pathology in a tubercle granuloma. However, it is still possible that although Th1 cells and CAMs control granuloma development initially, later in the process Th2 cells and AAMs are activated to induce fibrosis and wall off the infection (Hogaboam et al., 1998; Wangoo et al., 2001).

The findings presented in this paper demonstrate that AAMs contribute to the inability of helminth-infected mice to control Mtb infection. Nevertheless, the precise mechanism of how AAMs support Mtb growth in vivo is less clear. Comparison of the transcriptional response to Mtb infection of BM macrophages activated with IL-4 or IFN-γ showed that alternative activation led to reduced nitrosative stress and increased iron availability (Kahnert et al., 2006), an environment conducive for Mtb growth. AAMs are characterized by the up-regulation of the mannose receptor (Gordon, 2003; Mosser, 2003) and Mtb can use the mannose receptor to gain entry into macrophages (Schlesinger, 1993). Although we did not see enhanced Mtb uptake by AAMs in vitro, further studies using fluorescently tagged Mtb and flow cytometric sorting of cells from infected lungs may help to enumerate Mtb numbers within distinct macrophage subsets. Transfer of WT macrophages into IL-4Rα$^{-/-}$ animals enhanced host susceptibility to Mtb, but whether reciprocal transfer of IL-4Rα$^{-/-}$ macrophages into WT mice will enhance resistance needs to be investigated. Additionally, further probing of the reciprocal transfer system with macrophages that are deficient in genes involved in AAM differentiation will allow us to precisely define the mechanism by which AAMs compromise protection against Mtb.

Macrophages exposed in vitro to Th2 cytokines are less efficient in killing intracellular Mtb because their autophagy pathway is blocked (Harris et al., 2007). Therefore, it is possible that the Th2 response induced in co-infected animals during early infection extends the duration of the AAM phenotype of the lung, allowing Mtb to resist autophagy-mediated killing for a longer time than what would occur in animals infected with Mtb alone. Furthermore, it is possible that as the Th2 response wanes and Th1 cytokines take over, the AAMs are able to undergo IFN-γ–mediated autophagy and Mtb killing. However, it remains to be determined whether in vivo AAMs can switch to CAMs or whether AAMs undergo apoptosis and the released bacteria are taken up by CAMs. In this context, a recent study (Day et al., 2009) describes a mathematical model that considers the interaction of Mtb with both AAMs and CAMs. Baseline simulation information with this model indicates that the switching time from AAM to CAM in the lung compartment during early infection can dictate the final outcome of infection. Similar modeling may be applied to develop a better understanding of how the Th2/Th1 balance of cytokines in the co-infected animals controls the AAM to CAM switching within the lung environment.

In vitro studies have shown that virulent strains of Mtb can induce the production of Th2 cytokines, whereas avirulent strains tend to elicit Th1 cytokines (Manca et al., 2004; Freeman et al., 2006; Rook, 2007). Furthermore, individuals with latent Mtb infection express elevated levels of the IL-4 antagonist IL-4Δ2 compared with both TB patients and uninfected individuals (Fletcher et al., 2004), suggesting that Th2 cytokines may undermine Th1-mediated immunity in TB patients. Indeed, neutralization of IL-4 either early or late during mouse Mtb infection led to significant reduction in lung bacterial burden (Buccheri et al., 2007; Roy et al., 2008). These studies, viewed in the broader context of disease susceptibility, suggest that to gain a better niche in the host, Mtb might either exploit the presence of preexisting AAMs in the lungs induced by helminth infections or itself promote AAM development via induction of Th2 cytokines. In conclusion, our study demonstrates that helminth infections compromise host resistance against Mtb and proposes that AAM induction is one mechanism through which helminth-induced Th2 cytokines impinge on immune control of Mtb.

MATERIALS AND METHODS

Mice. BALB/c mice and breeding pairs of IL-4Rα$^{-/-}$ mice were purchased from The Jackson Laboratory. Breeding of IL-4Rα$^{-/-}$ mice was done at the transgenic animal barrier facility at the University of Medicine and Dentistry of New Jersey. All animal studies were approved by the Institutional Animal Care and Use Committee.

Parasite isolation and inoculation. Isolation of Nb larvae was performed as previously described (Liu et al., 2002). In brief, parasite eggs shed with the feces of Nb-infected BALB/c mice were cultured in a mixture of charcoal and sphagnum moss stored in plastic Petri dishes, which allows eggs to develop into the L3 stage infective larvae within 1 wk. Mice were inoculated subcutaneously in the area of the axillary fat pad with a 100-µl suspension of 500 L3 larvae collected from cultures using a modified Baermann apparatus.

Mtb growth assay. BMDMs were prepared as described previously (Bhatt et al., 2004). On day 7, BMDMs from WT mice were harvested and plated in 24-well plates (Corning) at a cell density of 2.5×10^5 cells/well in antibiotic-free DME containing 10% FBS (D-10). BMDMs were left untreated, or stimulated with 20 ng/ml IL-4 + 10 ng/ml IL-13 (BD) or 100 U/ml IFN-γ (PeproTech) for 16 h. Cells were infected with Erdman Mtb at an MOI of 1 for 5 h. Media was then removed and replaced with D-10 containing 200 µg/ml amikacin (Sigma-Aldrich) for 1 h, after which wells were washed 3× with PBS + 1% BCS. Some of the IL-4 + IL-13–treated macrophages received 100 U/ml IFN-γ. Cultures were maintained in D-10 media containing 1% L-cell supernatants and replaced every 2 d. At the indicated time points, wells were washed and cells lysed with 1 ml sterile H_2O. Lysates were serially diluted in PBS + 0.05% Tween-80 for CFU determination and 100 µl was plated in duplicate. Plates were counted after incubation at 37°C for 14 d.

Aerosol infection, CFU determination, preparation of single cell suspension, RNA isolation, and histological analysis. Aerosol infection with Erdman Mtb (Trudeau Institute) of BALB/c female mice (6–8 wk old) was performed in a closed-air aerosolization system (In-Tox Products). Mice were exposed for 20 min to nebulized Mtb at a density which was optimized to deliver a low dose of ∼100 CFU to the lungs. At each time interval studied, infected animals were sacrificed by cervical dislocation and the right superior lobe of the lung was homogenized in PBS containing 0.05% Tween-80. Serial dilutions of the homogenates were plated onto 7H11 agar. The plates were incubated at 37°C and colonies counted after 21 d. For histology,

the left lobe of each infected lung was fixed in 4% PFA for 5 d, 70% ethanol overnight, and subsequently embedded in paraffin. For pathology analysis, sections were stained with hematoxylin and eosin. For RNA isolation, the postcaval lobe was removed, homogenized in 2 ml TRIzol reagent (Invitrogen) and stored at −80°C. Single-cell suspensions of draining LNs and lung cells were prepared as previously described (Bhatt et al., 2004). For obtaining single cell suspensions, the lungs were perfused with 5 ml sterile PBS and harvested. Mediastinal LNs were also harvested and both tissues were processed separately to obtain single cell suspensions. Lungs were cut into small pieces and incubated with 1 mg/ml collagenase D (Roche) for 30 min. The digestion was stopped by adding 5 mM EDTA. The digested tissue was transferred to a 40-μM nylon cell strainer and disrupted using a syringe plunger to obtain single cell suspensions. LN tissue was processed similarly, but without collagenase digestion. RBCs were lysed with ACK lysis buffer and viable cell number was determined by trypan blue dye exclusion.

ELISPOT. Single-cell suspensions of draining LNs and lung cells were prepared as described in the previous section. Cells were cultured in DME supplemented with 5% L-glutamine, 25 mM HEPES, 10% FBS, and 50 μM 2-ME. ELISPOT assay was performed according to previously described protocol (Lazarevic et al., 2005). Lung and LN cells were plated either in 5 μg/ml anti–IFN-γ (BD) or 5 μg/ml anti–IL-4 (BD) coated ELISPOT plates (Millipore). Cells were co-cultured at a 1:2 ratio with either uninfected or Mtb-infected dendritic cells (multiplicity of infection of three) to estimate the total number of Mtb-specific IFN-γ and IL-4–producing T cells. BM-derived dendritic cells were prepared as described previously (Bhatt et al., 2004). All cultures were supplemented with IL-2 at a final concentration of 20 U/ml and were incubated for 40 h. For detection of total IL-4–secreting cells, cultures were stimulated with 1 μg/ml of plate-bound anti-CD3 (BD) and 0.2 μg/ml anti-CD28 (BD) for 24 h. For spot visualization, plates were first incubated with biotinylated anti–IFN-γ (BD) or anti–IL-4 (BD), and then streptavidin-conjugated peroxidase (BD) and finally 3-amino-9-ethylcarbazole substrate (Sigma-Aldrich). The spot-forming units were counted using an ELISPOT reader (Cellular Technology).

RNA purification, cDNA synthesis, and real-time PCR. Total RNA was purified using TRIzol reagent and chloroform extraction, followed by precipitation in isopropyl alcohol and 70% ethanol. RNA was purified using the RNeasy purification kit (QIAGEN). cDNA synthesis was performed using the Superscript II protocol (Invitrogen). Real-time PCR was performed in the Mx3000p thermal cycler (Agilent Technologies) using SYBR Green chemistry. The reactions were performed to generate cycles (Ct). Using the comparative Ct method relative gene expression was calculated as $2^{(-\Delta\Delta Ct)}$, where ΔCt = Ct (gene of interest) − Ct (normalizer = β-actin) and the $\Delta\Delta Ct = \Delta Ct$ (sample) − ΔCt (calibrator). Calibrator was total RNA from uninfected lung or LN. Data are expressed as mean ± SD.

Immunohistochemistry. Immunohistochemistry for NOS2 and ARG-1 protein was performed on formalin-fixed paraffin-embedded lung sections. Samples were deparaffinized, rehydrated, and processed for Ag retrieval. To detect NOS2 protein, sections were subjected to microwave antigen retrieval in citrate buffer. For ARG-1 protein, antibody epitopes were unmasked by 20-min incubation in PBS-0.5% Tween-20 at room temperature. Endogenous peroxidase activity was blocked by 15-min incubation in 3% H_2O_2 followed by blocking for avidin and biotin using a commercial reagent (Vector Laboratories). For primary staining, sections were incubated overnight at 4°C with the mouse anti–arginase-1 (clone 19) or mouse anti–Nos-2 (clone 6; BD) and detected using the Vector M.O.M Immunodetection kit (Vector Laboratories) according to manufacturer recommendations. Bound antibody was visualized by diaminobenzidine followed by a hematoxylin counterstain.

Flow cytometry. Single cell suspensions from lungs of infected animals were washed with PBS containing 2% BCS and 0.09% sodium azide (FACS buffer). Cells were incubated with purified anti-CD16/CD32 (2.4G2; BD) to inhibit nonspecific staining and stained for CD11b-PE (M1/70) and CD11c-APC (HL3; BD). Cells were fixed in 4% paraformaldehyde, blocked, and permeabilized for 30 min with PBST (PBS, 0.3% Triton X-100, 1% BSA, and 1% goat serum) at room temperature and simultaneously stained for intracellular NOS2 and Fizz1 expression. Anti–NOS2-FITC was purchased from BD. Fizz1 was detected using a biotinylated polyclonal antibody (Abcam), followed by PE-Cy7 streptavidin (BD; Shirey et al., 2008). Cells were washed with PBST and fixed in 2% paraformaldehyde in PBS for FACS analysis. Cells were collected using a LSRII flow cytometer (BD) and analyzed using FlowJo software (version 6.4; Tree Star). All gates and quadrants were set using relevant isotype control antibodies.

Determination of arginase activity. Arginase activity was determined by measuring the total production of urea from lung homogenates. Lysates were filtered through 0.22-μm centrifuge filters (Millipore) and urea levels were determined using a QuantiChrom Arginase Assay kit (BioAssay Sytems). Arginase activity is expressed as units per liter of ample, where 1 unit of arginase converts 1 μmole of L-arginine to ornithine and urea per minute at pH 9.5 and 37°C.

Adoptive transfer of macrophages. Peritoneal exudate macrophages (PEM) from WT and IL-4Rα$^{-/-}$ mice (five mice/group) were elicited by an intraperitoneal injection of 2 ml sterile thioglycollate broth 5 d before peritoneal lavage. PEM from each group of mice was pooled and IL-4Rα$^{-/-}$ mice received 10×10^6 WT or IL-4Rα$^{-/-}$ macrophages via the intratracheal route as previously described (Bhatt et al., 2004).

Statistics. For statistical analysis of samples, Student's *t* tests and ANOVA were performed (PRISM version 4.0; GraphPad Software) as appropriate. Values of $P < 0.05$ were considered significant.

Online supplemental material. Fig. S1 is a representative flow cytometry dot plot of the distribution of $Cd11b^+c^-$, $CD11b^-c^+$, and $CD11b^+c^+$ cells in lung cells of Mtb-infected mice. Figs. S2 and S3 display the quantification of NOS2- and Fizz-1–expressing cells, respectively. Fig. S4 shows in absolute numbers the survival of the intratracheally instilled CFSE-labeled peritoneal macrophages in the lungs. Online supplemental material is available at http://www.jem.org/cgi/content/full/jem.20091473/DC1.

This work was supported by National Institutes of Health Grant AI 069395 to PS and WCG and AI075859 to JP.

The authors have no conflicting financial interests.

Submitted: 8 July 2009
Accepted: 19 July 2011

REFERENCES

Actor, J.K., M. Shirai, M.C. Kullberg, R.M. Buller, A. Sher, and J.A. Berzofsky. 1993. Helminth infection results in decreased virus-specific CD8+ cytotoxic T-cell and Th1 cytokine responses as well as delayed virus clearance. *Proc. Natl. Acad. Sci. USA*. 90:948–952. doi:10.1073/pnas.90.3.948

Anthony, R.M., L.I. Rutitzky, J.F. Urban Jr., M.J. Stadecker, and W.C. Gause. 2007. Protective immune mechanisms in helminth infection. *Nat. Rev. Immunol.* 7:975–987. doi:10.1038/nri2199

Arora, S., Y. Hernandez, J.R. Erb-Downward, R.A. McDonald, G.B. Toews, and G.B. Huffnagle. 2005. Role of IFN-gamma in regulating T2 immunity and the development of alternatively activated macrophages during allergic bronchopulmonary mycosis. *J. Immunol.* 174:6346–6356.

Babu, S., S.Q. Bhat, N.P. Kumar, S. Jayantasri, S. Rukmani, P. Kumaran, P.G. Gopi, C. Kolappan, V. Kumaraswami, and T.B. Nutman. 2009. Human type 1 and 17 responses in latent tuberculosis are modulated by coincident filarial infection through cytotoxic T lymphocyte antigen-4 and programmed death-1. *J. Infect. Dis.* 200:288–298. doi:10.1086/599797

Bethony, J., S. Brooker, M. Albonico, S.M. Geiger, A. Loukas, D. Diemert, and P.J. Hotez. 2006. Soil-transmitted helminth infections: ascariasis, trichuriasis, and hookworm. *Lancet*. 367:1521–1532. doi:10.1016/S0140-6736(06)68653-4

Bhatt, K., S.P. Hickman, and P. Salgame. 2004. Cutting edge: a new approach to modeling early lung immunity in murine tuberculosis. *J. Immunol.* 172:2748–2751.

Brooker, S., A.C. Clements, and D.A. Bundy. 2006. Global epidemiology, ecology and control of soil-transmitted helminth infections. *Adv. Parasitol.* 62:221–261. doi:10.1016/S0065-308X(05)62007-6

Buccheri, S., R. Reljic, N. Caccamo, J. Ivanyi, M. Singh, A. Salerno, and F. Dieli. 2007. IL-4 depletion enhances host resistance and passive IgA protection against tuberculosis infection in BALB/c mice. *Eur. J. Immunol.* 37:729–737. doi:10.1002/eji.200636764

Chan, J., Y. Xing, R.S. Magliozzo, and B.R. Bloom. 1992. Killing of virulent *Mycobacterium tuberculosis* by reactive nitrogen intermediates produced by activated murine macrophages. *J. Exp. Med.* 175:1111–1122. doi:10.1084/jem.175.4.1111

Co, D.O., L.H. Hogan, S.I. Kim, and M. Sandor. 2004. Mycobacterial granulomas: keys to a long-lasting host-pathogen relationship. *Clin. Immunol.* 113:130–136. doi:10.1016/j.clim.2004.08.012

Day, J., A. Friedman, and L.S. Schlesinger. 2009. Modeling the immune rheostat of macrophages in the lung in response to infection. *Proc. Natl. Acad. Sci. USA.* 106:11246–11251. doi:10.1073/pnas.0904846106

El Kasmi, K.C., J.E. Qualls, J.T. Pesce, A.M. Smith, R.W. Thompson, M. Henao-Tamayo, R.J. Basaraba, T. König, U. Schleicher, M.S. Koo, et al. 2008. Toll-like receptor-induced arginase 1 in macrophages thwarts effective immunity against intracellular pathogens. *Nat. Immunol.* 9:1399–1406. doi:10.1038/ni.1671

Elias, D., H. Akuffo, A. Pawlowski, M. Haile, T. Schön, and S. Britton. 2005. *Schistosoma mansoni* infection reduces the protective efficacy of BCG vaccination against virulent *Mycobacterium tuberculosis*. *Vaccine*. 23:1326–1334. doi:10.1016/j.vaccine.2004.09.038

Elias, D., S. Britton, A. Aseffa, H. Engers, and H. Akuffo. 2008. Poor immunogenicity of BCG in helminth infected population is associated with increased in vitro TGF-beta production. *Vaccine*. 26:3897–3902. doi:10.1016/j.vaccine.2008.04.083

Fletcher, H.A., P. Owiafe, D. Jeffries, P. Hill, G.A. Rook, A. Zumla, T.M. Doherty, and R.H. Brookes; Vacsel Study Group. 2004. Increased expression of mRNA encoding interleukin (IL)-4 and its splice variant IL-4delta2 in cells from contacts of Mycobacterium tuberculosis, in the absence of in vitro stimulation. *Immunology*. 112:669–673. doi:10.1111/j.1365-2567.2004.01922.x

Freeman, S., F.A. Post, L.G. Bekker, R. Harbacheuski, L.M. Steyn, B. Ryffel, N.D. Connell, B.N. Kreiswirth, and G. Kaplan. 2006. Mycobacterium tuberculosis H37Ra and H37Rv differential growth and cytokine/chemokine induction in murine macrophages in vitro. *J. Interferon Cytokine Res.* 26:27–33. doi:10.1089/jir.2006.26.27

Gordon, S. 2003. Alternative activation of macrophages. *Nat. Rev. Immunol.* 3:23–35. doi:10.1038/nri978

Harris, J., S.A. De Haro, S.S. Master, J. Keane, E.A. Roberts, M. Delgado, and V. Deretic. 2007. T helper 2 cytokines inhibit autophagic control of intracellular *Mycobacterium tuberculosis*. *Immunity*. 27:505–517. doi:10.1016/j.immuni.2007.07.022

Harvie, M., M. Camberis, S.C. Tang, B. Delahunt, W. Paul, and G. Le Gros. 2010. The lung is an important site for priming CD4 T-cell-mediated protective immunity against gastrointestinal helminth parasites. *Infect. Immun.* 78:3753–3762. doi:10.1128/IAI.00502-09

Helmby, H., M. Kullberg, and M. Troye-Blomberg. 1998. Altered immune responses in mice with concomitant *Schistosoma mansoni* and *Plasmodium chabaudi* infections. *Infect. Immun.* 66:5167–5174.

Herbert, D.R., C. Hölscher, M. Mohrs, B. Arendse, A. Schwegmann, M. Radwanska, M. Leeto, R. Kirsch, P. Hall, H. Mossmann, et al. 2004. Alternative macrophage activation is essential for survival during schistosomiasis and downmodulates T helper 1 responses and immunopathology. *Immunity*. 20:623–635. doi:10.1016/S1074-7613(04)00107-4

Hogaboam, C.M., C.S. Gallinat, C. Bone-Larson, S.W. Chensue, N.W. Lukacs, R.M. Strieter, and S.L. Kunkel. 1998. Collagen deposition in a non-fibrotic lung granuloma model after nitric oxide inhibition. *Am. J. Pathol.* 153:1861–1872. doi:10.1016/S0002-9440(10)65700-8

Hölscher, C., B. Arendse, A. Schwegmann, E. Myburgh, and F. Brombacher. 2006. Impairment of alternative macrophage activation delays cutaneous leishmaniasis in nonhealing BALB/c mice. *J. Immunol.* 176:1115–1121.

Hsieh, C.-S., S.E. Macatonia, C.S. Tripp, S.F. Wolf, A. O'Garra, and K.M. Murphy. 1993. Development of TH1 CD4+ T cells through IL-12 produced by *Listeria*-induced macrophages. *Science*. 260:547–549. doi:10.1126/science.8097338

Jankovic, D., M.C. Kullberg, N. Noben-Trauth, P. Caspar, W.E. Paul, and A. Sher. 2000. Single cell analysis reveals that IL-4 receptor/Stat6 signaling is not required for the in vivo or in vitro development of CD4+ lymphocytes with a Th2 cytokine profile. *J. Immunol.* 164:3047–3055.

Jung, Y.J., R. LaCourse, L. Ryan, and R.J. North. 2002. Evidence inconsistent with a negative influence of T helper 2 cells on protection afforded by a dominant T helper 1 response against *Mycobacterium tuberculosis* lung infection in mice. *Infect. Immun.* 70:6436–6443. doi:10.1128/IAI.70.11.6436-6443.2002

Kahnert, A., P. Seiler, M. Stein, S. Bandermann, K. Hahnke, H. Mollenkopf, and S.H. Kaufmann. 2006. Alternative activation deprives macrophages of a coordinated defense program to *Mycobacterium tuberculosis*. *Eur. J. Immunol.* 36:631–647. doi:10.1002/eji.200535496

Lazarevic, V., S. Pawar, and J. Flynn. 2005. Measuring T-cell function in animal models of tuberculosis by ELISPOT. *Methods Mol. Biol.* 302:179–190.

Le Gros, G., S.Z. Ben-Sasson, R. Seder, F.D. Finkelman, and W.E. Paul. 1990. Generation of interleukin 4 (IL-4)–producing cells in vivo and in vitro: IL-2 and IL-4 are required for in vitro generation of IL-4–producing cells. *J. Exp. Med.* 172:921–929. doi:10.1084/jem.172.3.921

Liu, Z., Q. Liu, J. Pesce, J. Whitmire, M.J. Ekkens, A. Foster, J. VanNoy, A.H. Sharpe, J.F. Urban Jr., and W.C. Gause. 2002. *Nippostrongylus brasiliensis* can induce B7-independent antigen-specific development of IL-4-producing T cells from naive CD4 T cells in vivo. *J. Immunol.* 169:6959–6968.

Loke, P., I. Gallagher, M.G. Nair, X. Zang, F. Brombacher, M. Mohrs, J.P. Allison, and J.E. Allen. 2007. Alternative activation is an innate response to injury that requires CD4+ T cells to be sustained during chronic infection. *J. Immunol.* 179:3926–3936.

MacMicking, J.D., R.J. North, R. LaCourse, J.S. Mudgett, S.K. Shah, and C.F. Nathan. 1997. Identification of nitric oxide synthase as a protective locus against tuberculosis. *Proc. Natl. Acad. Sci. USA.* 94:5243–5248. doi:10.1073/pnas.94.10.5243

Malhotra, I., P. Mungai, A. Wamachi, J. Kioko, J.H. Ouma, J.W. Kazura, and C.L. King. 1999. Helminth- and Bacillus Calmette-Guérin-induced immunity in children sensitized in utero to filariasis and schistosomiasis. *J. Immunol.* 162:6843–6848.

Manca, C., M.B. Reed, S. Freeman, B. Mathema, B. Kreiswirth, C.E. Barry III, and G. Kaplan. 2004. Differential monocyte activation underlies strain-specific *Mycobacterium tuberculosis* pathogenesis. *Infect. Immun.* 72:5511–5514. doi:10.1128/IAI.72.9.5511-5514.2004

Marsland, B.J., M. Kurrer, R. Reissmann, N.L. Harris, and M. Kopf. 2008. *Nippostrongylus brasiliensis* infection leads to the development of emphysema associated with the induction of alternatively activated macrophages. *Eur. J. Immunol.* 38:479–488. doi:10.1002/eji.200737827

Martinez, F.O., L. Helming, and S. Gordon. 2009. Alternative activation of macrophages: an immunologic functional perspective. *Annu. Rev. Immunol.* 27:451–483. doi:10.1146/annurev.immunol.021908.132532

McKee, A.S., and E.J. Pearce. 2004. CD25+CD4+ cells contribute to Th2 polarization during helminth infection by suppressing Th1 response development. *J. Immunol.* 173:1224–1231.

Mosser, D.M. 2003. The many faces of macrophage activation. *J. Leukoc. Biol.* 73:209–212. doi:10.1189/jlb.0602325

Mosser, D.M., and J.P. Edwards. 2008. Exploring the full spectrum of macrophage activation. *Nat. Rev. Immunol.* 8:958–969. doi:10.1038/nri2448

Müller, U., W. Stenzel, G. Köhler, C. Werner, T. Polte, G. Hansen, N. Schütze, R.K. Straubinger, M. Blessing, A.N. McKenzie, et al. 2007. IL-13 induces disease-promoting type 2 cytokines, alternatively activated macrophages and allergic inflammation during pulmonary infection of mice with *Cryptococcus neoformans*. *J. Immunol.* 179:5367–5377.

Pearlman, E., J.W. Kazura, F.E. Hazlett Jr., and W.H. Boom. 1993. Modulation of murine cytokine responses to mycobacterial antigens by helminth-induced T helper 2 cell responses. *J. Immunol.* 151:4857–4864.

Qualls, J.E., G. Neale, A.M. Smith, M.S. Koo, A.A. DeFreitas, H. Zhang, G. Kaplan, S.S. Watowich, and P.J. Murray. 2010. Arginine usage in mycobacteria-infected macrophages depends on autocrine-paracrine cytokine signaling. *Sci. Signal.* 3:ra62. doi:10.1126/scisignal.2000955

Reece, J.J., M.C. Siracusa, T.L. Southard, C.F. Brayton, J.F. Urban Jr., and A.L. Scott. 2008. Hookworm-induced persistent changes to the immunological environment of the lung. *Infect. Immun.* 76:3511–3524. doi:10.1128/IAI.00192-08

Resende Co, T., C.S. Hirsch, Z. Toossi, R. Dietze, and R. Ribeiro-Rodrigues. 2007. Intestinal helminth co-infection has a negative impact on both anti-*Mycobacterium tuberculosis* immunity and clinical response to tuberculosis therapy. *Clin. Exp. Immunol.* 147:45–52.

Rodríguez, M., L.I. Terrazas, R. Márquez, and R. Bojalil. 1999. Susceptibility to *Trypanosoma cruzi* is modified by a previous non-related infection. *Parasite Immunol.* 21:177–185. doi:10.1046/j.1365-3024.1999.00218.x

Rook, G.A. 2007. Th2 cytokines in susceptibility to tuberculosis. *Curr. Mol. Med.* 7:327–337. doi:10.2174/156652407780598557

Roy, E., J. Brennan, S. Jolles, and D.B. Lowrie. 2008. Beneficial effect of anti-interleukin-4 antibody when administered in a murine model of tuberculosis infection. *Tuberculosis* (*Edinb.*). 88:197–202. doi:10.1016/j.tube.2007.11.005

Satoh, T., O. Takeuchi, A. Vandenbon, K. Yasuda, Y. Tanaka, Y. Kumagai, T. Miyake, K. Matsushita, T. Okazaki, T. Saitoh, et al. 2010. The Jmjd3-Irf4 axis regulates M2 macrophage polarization and host responses against helminth infection. *Nat. Immunol.* 11:936–944. doi:10.1038/ni.1920

Schlesinger, L.S. 1993. Macrophage phagocytosis of virulent but not attenuated strains of *Mycobacterium tuberculosis* is mediated by mannose receptors in addition to complement receptors. *J. Immunol.* 150:2920–2930.

Seder, R.A., R. Gazzinelli, A. Sher, and W.E. Paul. 1993. Interleukin 12 acts directly on CD4+ T cells to enhance priming for interferon gamma production and diminishes interleukin 4 inhibition of such priming. *Proc. Natl. Acad. Sci. USA.* 90:10188–10192. doi:10.1073/pnas.90.21.10188

Sher, A., D. Fiorentino, P. Caspar, E. Pearce, and T. Mosmann. 1991. Production of IL-10 by CD4+ T lymphocytes correlates with down-regulation of Th1 cytokine synthesis in helminth infection. *J. Immunol.* 147:2713–2716.

Shirey, K.A., L.E. Cole, A.D. Keegan, and S.N. Vogel. 2008. Francisella tularensis live vaccine strain induces macrophage alternative activation as a survival mechanism. *J. Immunol.* 181:4159–4167.

Stewart, G.R., M. Boussinesq, T. Coulson, L. Elson, T. Nutman, and J.E. Bradley. 1999. Onchocerciasis modulates the immune response to mycobacterial antigens. *Clin. Exp. Immunol.* 117:517–523. doi:10.1046/j.1365-2249.1999.01015.x

Tumitan, A.R., L.G. Monnazzi, F.R. Ghiraldi, E.M. Cilli, and B.M. Machado de Medeiros. 2007. Pattern of macrophage activation in yersinia-resistant and yersinia-susceptible strains of mice. *Microbiol. Immunol.* 51:1021–1028.

van Panhuys, N., S.C. Tang, M. Prout, M. Camberis, D. Scarlett, J. Roberts, J. Hu-Li, W.E. Paul, and G. Le Gros. 2008. In vivo studies fail to reveal a role for IL-4 or STAT6 signaling in Th2 lymphocyte differentiation. *Proc. Natl. Acad. Sci. USA.* 105:12423–12428. doi:10.1073/pnas.0806372105

Wangoo, A., T. Sparer, I.N. Brown, V.A. Snewin, R. Janssen, J. Thole, H.T. Cook, R.J. Shaw, and D.B. Young. 2001. Contribution of Th1 and Th2 cells to protection and pathology in experimental models of granulomatous lung disease. *J. Immunol.* 166:3432–3439.

Weng, M., D. Huntley, I.F. Huang, O. Foye-Jackson, L. Wang, A. Sarkissian, Q. Zhou, W.A. Walker, B.J. Cherayil, and H.N. Shi. 2007. Alternatively activated macrophages in intestinal helminth infection: effects on concurrent bacterial colitis. *J. Immunol.* 179:4721–4731.

World Health Organization. 2008. Global Tuberculosis Control-Surveillance, Planning, Financing. WHO Press, Geneva, Switzerland. 294 pp.